



HAL
open science

Electronic structure of $\text{Ln}_2\text{O}_2\text{Te}$ ($\text{Ln}=\text{La}$, Sm and Gd) by X-ray absorption spectroscopy

S. Gautam, K.H. Chae, J. Llanos, O. Peña, K. Asokan

► **To cite this version:**

S. Gautam, K.H. Chae, J. Llanos, O. Peña, K. Asokan. Electronic structure of $\text{Ln}_2\text{O}_2\text{Te}$ ($\text{Ln}=\text{La}$, Sm and Gd) by X-ray absorption spectroscopy. *Vacuum*, 2018, 158, pp.39-41. 10.1016/j.vacuum.2018.09.008 . hal-01905104

HAL Id: hal-01905104

<https://univ-rennes.hal.science/hal-01905104v1>

Submitted on 14 Dec 2018

HAL is a multi-disciplinary open access archive for the deposit and dissemination of scientific research documents, whether they are published or not. The documents may come from teaching and research institutions in France or abroad, or from public or private research centers.

L'archive ouverte pluridisciplinaire **HAL**, est destinée au dépôt et à la diffusion de documents scientifiques de niveau recherche, publiés ou non, émanant des établissements d'enseignement et de recherche français ou étrangers, des laboratoires publics ou privés.

Electronic Structure of $\text{Ln}_2\text{O}_2\text{Te}$ ($\text{Ln}=\text{La}$, Sm and Gd) by X-ray Absorption Spectroscopy

Sanjeev Gautam^{a,*}, Keun Hwa Chae^b, Jaime Llanos^c, Octavio Peña^d, K. Asokan^e

^a*Dr. S.S. Bhatnagar University Institute of Chemical Engineering & Technology, Panjab University, Chandigarh 160-014, India*

^b*Advanced Analysis Center, Korea Institute of Science and Technology, Seoul 136-791, Republic of Korea*

^c*Departamento de Química, Universidad Católica del Norte, Avda. Angamos 0610, Casilla 1280, Antofagasta, Chile*

^d*Institut de Sciences Chimiques de Rennes/UMR 6226, Université de Rennes 1, 35042 Rennes Cedex, France*

^e*Inter University Accelerator Center, Aruna Asaf Ali Marg, New Delhi 110-067, India*

Abstract

The oxytelluride are layered structure materials shows low lattice thermal conductivity and hence making them suitable for high temperature thermoelectric materials. We report the electronic structural properties of rare-earth doped oxytellurides [$\text{Ln}_2\text{O}_2\text{Te}$ ($\text{Ln}=\text{La}$, Sm and Gd)] prepared by solid state reaction method. This research is focused on the suitability of rare-earth oxychalcogenide as a thermoelectric material using electronic structure investigations. The X-ray absorption spectra at O K-edge show the O $2p$ bonding with Ln $5d$ and $4f$ and Te $5s$ states and the Ln M-edges show that the valences of Ln are to be trivalent or mixed state. The Ln M-edges are also simulated with Cowan code, and electronic structures of these oxytellurides are discussed. The substitution of different rare earth metals at the Ln-site, may enhance the thermoelectric property and stability of the material.

Keywords: Rare earth alloys and compounds, NEXAFS, synchrotron radiation

PACS: 71.20.Eh, 78.70.Dm

*Corresponding author: Phone/Fax: ++91-9779713212,
Email address: sgautam@pu.ac.in (Sanjeev Gautam)

1. Introduction

The rare-earth based oxychalcogenides belong to the group of compounds with oxygen, sulfur, selenium, and tellurium. Rare earth chalcogenides with high oxygen concentration result in a distinct and nearly stoichiometric oxychalcogenides, $\text{Ln}_2\text{O}_2\text{X}$ ($\text{X} = \text{S}, \text{Se}, \text{Te}$). These compounds have many interesting optical, electrical, magnetic and thermoelectric properties and are very promising candidates for many diverse practical applications in lasers, wide gap electro-luminescent devices, LED phosphors and scintillation detectors [1, 2, 3].

Surprisingly, few studies have been carried out in these compounds especially in oxytellurides due to technical difficulties in the sample preparation. The rare-earth oxytellurides, $\text{Ln}_2\text{O}_2\text{Te}$ ($\text{Ln} = \text{La-Nd}$ and Sm-Ho) crystalizes in the tetragonal crystal structure, space group $I4/mmm$ (space group 139) with two(2) formulas per unit cell [2, 4]. Such a crystal structure is an anti- ThCr_2Si_2 -type, where the Ln^{3+} positive ions are surrounded by eight -ve ions (4O^{2-} and 4Te^{2-}) in a distorted square antiprism structure. These polyhedra are links together in manner that provides a well maintained crystal structure along with charge balance [4]. If the rule of electron counting is followed, then the oxidation states of Ln, O and Te are expected to be 3+, 2- and 2-, respectively. Llanos *et al.* have also investigated the magnetic, optical properties along with electronic structure of $\text{Ln}_2\text{O}_2\text{Te}$ ($\text{Ln}=\text{La}, \text{Sm}$ and Gd) [4].

The rare-earth oxychalcogenides have a similar electronic structure as compared to $\text{Bi}_2\text{O}_2\text{X}$ ($\text{X}=\text{Se}, \text{Te}$), whose lattice thermal conductivity is of the range of the glass like structure. So, there is a possibility that $\text{Ln}_2\text{O}_2\text{Te}$ ($\text{Ln}=\text{La}, \text{Sm}$ and Gd) should show a similar behavior[5]. The operating temperature of this structure is approximately 800 K because of the decomposition factor (~ 1200 K), which limits its temperature range. A suitable study of $\text{Ln}_2\text{O}_2\text{Te}$ ($\text{Ln}=\text{La}, \text{Sm}$ and Gd) , could give an idea to enhance the operating temperature and hence to make it a suitable candidate for high temperature thermoelectric material.

$\text{Bi}_2\text{O}_2\text{Te}$ material consists of $(\text{Bi}_2\text{O}_2)^{2+}$ layer and Te^{2-} square net layer, alternatively

arranged along the *c*-axis, making a layered structure material. The oxygen anions are tetrahedrally coordinated by 4 Bi cations at a distance of 2.3434 Å forming fluorite type slabs. Each Bi cation is at the center of the square antiprism, surrounded by 4 O and 4 Te anions. The reported figure of merit for Bi₂O₂Te is approx. 0.13 at 573 K because of the low charge carrier concentration [5, 6]. Hence, if the charge carrier concentration is enhanced, higher figure of merit can be achieved. Also, as the thermal conductivity decreases with increase in mean atomic weight, so replacing Bi-atom by a RE-metal may show even lower thermal conductivity as compared to Bi₂O₂Te and Bi₂O₂Se [7]. The modification in the electronic structure due to the substitution of rare-earth(RE) metal at Bi-site (Ln-site), could help in comprehending the variation in the thermoelectric properties.

Among the spectroscopic techniques, the near-edge X-ray absorption fine structure (NEXAFS) spectroscopy gives specific information about the unoccupied states. NEXAFS spectroscopy is an effective tool to study 4*f*-electronic states of rare-earth compounds and has clarified the origin of their unique behavior. This study provides information about electronic and atomic structure. Using these studies one can understand the bonding of O with rare-earth ions, valence of rare-earth ions and resulting electronic structure, which determines their optical and magnetic properties.

Present study focuses the electronic structure of Ln₂O₂Te (Ln=La, Sm and Gd) using NEXAFS spectroscopy with special reference to the nature of O 2*p* bonding and valence states of the rare-earth ions.

2. Experimental

Compounds reported in this paper were synthesized starting from the respective (Sigma Aldrich 99%) pure oxides (La₂O₃ Sm₂O₃ and Gd₂O₃) and elemental tellurium. The reactants, elemental tellurium and respective rare-earth oxides, were adjacently placed in an alumina boat and heated for 5 hrs under controlled hydrogen flow at 950 K. Sample preparation details are described in literature [4]. The crystalline phase and composition were analyzed using X-ray diffraction (XRD), and energy-dispersive spectroscopy (EDS), respectively [4]. For electronic structure investigation, NEXAFS measurements were carried out

at the 10D (XAS KIST) beamline of Pohang Accelerator Lab. (Pohang, South Korea) with 3 GeV energy and 300 mA storage ring current in top-up mode. These measurements were performed at ultra-high vacuum ($\sim 10^{-9}$ Torr) at 300 K (RT) with a beamline resolution about 0.6 eV at O K-edge energy. All spectra were normalized to the post-edge step height using Athena, after a constant background subtraction [8].

3. Results and discussion

3.1. Structural study

The XRD patterns of $\text{Ln}_2\text{O}_2\text{Te}$ (Ln=La, Sm and Gd) reflect the crystallinity and homogeneity of the prepared samples, as described in an earlier publication [4]. The crystal structure is discussed as an anti-isotype with ThCr_2Si_2 , where the Ln^{3+} +ve ions are surrounded by eight -ve ions (4O^{2-} and 4Te^{2-})[4, 9]. The highest intense peak for $\text{Ln}_2\text{O}_2\text{Te}$ (Ln=La, Sm and Gd) is observed at 30° . The experimental pattern agree with the calculated pattern from ICS database[10], which is also well supported as discussed by Llanos *et al.* and Weber *et al.* .

3.2. Electronic structure through NEXAFS

3.2.1. O K-edge NEXAFS

Figure 1 shows the normalized O K-edge NEXAFS spectra for $\text{Ln}_2\text{O}_2\text{Te}$ compounds. All the major spectral features at 529.5, 535, and 538.9 eV are marked as A_1 , B_1 and C_1 . In general, O K-edge spectrum provides information about the unoccupied O $2p$ states[11, 12]. Usually, rare earth oxides show two broad spectral features associated with O- $2p$ hybridization with Ln $5d$ states. Nachimuthu *et al.* and Lee *et al.* observed two broad peaks centered at 532 eV and 537 eV [13, 14]. As evident in the inset of Fig. 1, three major spectral features are clearly seen in this case of rare-earth tellurides. The post-edge feature (C_1) may be assigned to the complex hybridization of Ln $4f$ - $5d$ -states with O- $2p$ states. Based on the electronic configuration, in trivalent state, La has no electrons, Sm 5 electrons and Gd 7 electrons in the $4f$ level.

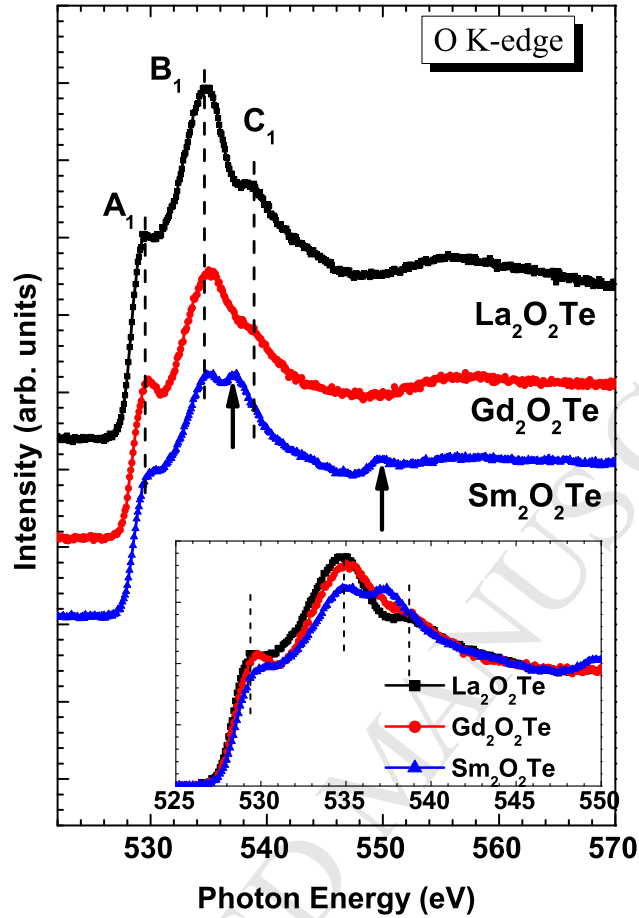


Figure 1: (Color online) Normalized NEXAFS spectra at O K-edge of $\text{Ln}_2\text{O}_2\text{Te}$ ($\text{Ln}=\text{La}, \text{Sm}$ and Gd) .

Sm is one the “anomalous” rare-earths (together with Ce , Eu and Yb) which may adopt two different valence states according to external parameters (pressure, temperature, stresses, etc.) or internal parameters (chemical pressure, stoichiometry, etc.) [15, 16]. C1 feature is representative of the mixed valence state, which is shown by Sm but not by La and Gd . Small C1 feature is also indicative of oxygen vacancy, which may be possible due to large La -series size. In contrast to this, the pre-edge feature (A_1) is highest for Gd and then decreases for Sm and La , respectively, which is direct evidence of $\text{O-}2p$ hybridization with $\text{Ln } 5d$ states. There is an extra feature seen for $\text{Sm}_2\text{O}_2\text{Te}$ as assigned by an up-arrow, at the post-edge, which may be due to the extra-vacancies in this compound responsible for large *Van Vleck* contribution as reported earlier [4, 17]. *Suljoti et al.* assign these peaks A_1 and

C_1 to Ln-O covalent bonding. The difference in their spectra may arise because of variation in crystal geometry, coordination numbers, and particle shape. Shifting of this peak towards the lower energy and strengthen across the series may indicate change of bonding and hence of valence state [18].

3.2.2. $M_{5,4}$ -edge NEXAFS

NEXAFS spectra at $M_{5,4}$ -edge on Ln-ions is a useful technique to comprehend the ground state $4f$ electron occupancy and hybridization state, which reveal the (average) valence state of the lanthanide ion[19]. Therefore, the $M_{5,4}$ -edge absorption spectra of lanthanide ions is collected by monitoring the lanthanide MNN Auger lines in a fixed energy window. The NEXAFS spectra for La/Sm/Gd M-edges as shown in Fig. 2 (a, b & c, resp.) shows two peaks positioned at 830, 845 eV and, 1075, 1105 eV, and, 1188, 1218 eV respectively. These peaks are assigned to the $3d-4f$ transition and the separation between the peaks is due to the spin-orbit splitting of the $3d_{5/2}(M_5)$ and $3d_{3/2}(M_4)$ level. The reason to the multiplet feature in each of the peaks is the spin-orbit moment coupling of $3d$ and $4f$ states [18, 20].

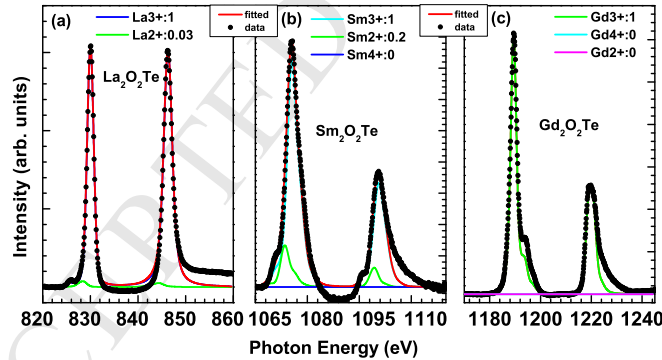


Figure 2: (Color online) Normalized NEXAFS spectra at (a) La $M_{5,4}$ -edge for $\text{La}_2\text{O}_2\text{Te}$, (b) Sm $M_{5,4}$ -edge for $\text{Sm}_2\text{O}_2\text{Te}$, and (c) Gd $M_{5,4}$ -edge for $\text{Gd}_2\text{O}_2\text{Te}$.

The $4f$ electrons in the lanthanides are screened from interatomic interaction of outer $5s$ and $5p$ orbital, owing to its overly localized nature. As a result of this, $4f$ orbital behaves as a strong centrifugal barrier in core-hole potential. Hence the contribution from the higher empty nf states ($n \geq 5$) in the absorption spectra is suppressed. On the other

hand, low density of the higher np empty states (below the conduction band) contribution is weak[20]. In view of the above, the $M_{5,4}$ -edge absorption spectra are mostly due to $3d^{10}4f^n \rightarrow 3d^9 4f^{n+1}$ electronic transitions. Every distinct M_5 and M_4 absorption line indicate a significant multiplet structure, which is governed by the Coulomb and exchange interaction between the $3d^9$ core hole and the $4f$ electrons (strong $4f$ shell localization) and the spin-orbit coupling of the core hole and $4f$ electrons ($j - j$ coupling), i.e., the fine structure is due to the intermediate coupling of the $3d^9$ hole and $4f$ electrons in the lanthanide ions.

The distinct fine structure and different intensity ratios between the multiplets is due to spin-orbit interaction between electrons of $4f$ -shell and exchange interaction between electrons of $3d$ holes and $4f$ electrons, which further depends upon the number present in the $4f$ shell. Therefore, the fine structure pattern of the $M_{5,4}$ -edge absorption spectra is an indication of the electronic configuration of the $4f$ subshell and which further unveils the (mean) oxidation state of the Ln-ions. The fine structure of the rare-earth oxychalcogenide samples obtained using X-ray absorption spectra is further strongly supported by Thole *et al.*, where they have used Cowan's atomic multiplet Hartree-Fock calculations with relativistic corrections [21] in the intermediate coupling, i.e., including all the states of the $4f^n$ configuration for the ground state and $3d^9 4f^{n+1}$ final state, for all the lanthanide ions and for all ionization states known in the solid state. This comparative study reveals that Ln-ions are in 3+ oxidation state, making ground state occupancy of $4f^0 - 4f^{13}$ for La to Yb.

In Figs. 2 (a,b & c), we have simulated the calculations for La, Sm and Gd-ions using Cowan code in CTM4XAS 5.0 as discussed by Thole *et al.*. The calculated NEXAFS spectra are compared with experimental data collected at the XAS beamline. In the case of La and Sm, an electronic ground state configuration of $4f^0$ and $4f^5$ is revealed respectively, while for Gd-ions an electronic ground state configuration of $4f^7$ is observed. Theoretical study indicates that the oxidation state of La and Gd-ions are +3, while mixed oxidation state of +2/+3 was observed in case of Sm-ions. The $M_{5,4}$ NEXAFS spectra were recorded in the electron yield (TEY) mode, which allows observation of surface induced valence changes due to its moderate surface sensitivity. Hence, it is predicted that due to a small crystallite size

of the samples, there is no surface induced valence changes.

The La/Sm/Gd M-edge spectrum in Figs.2 (a, b & c) involve pre-threshold peaks and a giant peak, in good agreement with the $4d-4f$ transition [22, 23]. The spectral features of La and Gd M-edges exhibit trivalent states and the Sm M-edges appear to indicate trivalent state or mixed valence state as the peak shape matches with trivalent state, with mixed feature of divalent and peak broadening [4, 18, 24].

4. Conclusions

The NEXAFS measurements at O K- and Ln M-edges provide the electronic structure of $\text{Ln}_2\text{O}_2\text{Te}$ (Ln=La, Sm and Gd) . La and Gd exist in trivalent state and Sm appears to be in trivalent or mixed valence state. In $\text{Bi}_2\text{O}_2\text{Te}$ system, Bi exists in +2 state. So, it is expected that rare-earth oxychalcogenide may show better electric conductivity than $\text{Bi}_2\text{O}_2\text{Te}$ system, because of higher charge carrier concentration. Oxygen and change in local symmetry may be the reason for enhanced magnetic properties in these materials as observed in other reports.

Acknowledgments

KA is thankful to Director, IUAC for encouragement and support. SG is thankful to thermoelectric applications expert *Kanika Upadhyay's* contribution in discussions. This research was supported by UGC-BSR research project.

REFERENCES

- [1] M. M. Lage, R. L. Moreira, F. M. Matinaga, J.-Y. Gesland, Chem. Mater. 17 (2005) 4523–4529.
- [2] M. Mikami, A. Oshiyama, Phys. Rev. B 57 (1998) 8939–8944.
- [3] H. Hiramatsu, K. Ueda, K. Takafuji, H. Ohta, M. Hirano, T. Kamiya, H. Hosono, J. Appl. Phys. 94 (2003) 5805–5808.
- [4] J. Llanos, S. Conejeros, R. Cortés, V. Sánchez, P. Barahona, O. Peña, Mat. Res. Bull. 43 (2008) 312 – 319.
- [5] S. D. Luu, P. Vaqueiro, Journal of Solid State Chemistry 226 (2015) 219–223.

- [6] P. Ruleova, C. Drasar, P. Lostak, C.-P. Li, S. Ballikaya, C. Uher, *Materials Chemistry and Physics* 119 (2010) 299–302.
- [7] G. S. Nolas, J. Sharp, J. Goldsmid, *Thermoelectrics: basic principles and new materials developments*, volume 45, Springer Science & Business Media, 2013.
- [8] B. Ravel, M. Newville, *J. Synch. Rad.* 12 (2005) 537–541.
- [9] A. Szytuła, B. Penc, M. Hofmann, J. Przewoźnik, *Solid State Communications* 152 (2012) 1027–1029.
- [10] ICSD (2/2005).
- [11] J. P. Singh, S. Gautam, P. Kumar, A. Tripathi, J.-M. Chen, K. H. Chae, K. Asokan, *J. Alloys Comp.* 572 (2013) 84 – 89.
- [12] A. Vij, S. Gautam, R. Kumar, A. K. Chawla, R. Chandra, N. Singh, K. H. Chae, *Journal of Alloys and Compounds* 527 (2012) 1 – 4.
- [13] P. Nachimuthu, S. Thevuthasan, M. H. Engelhard, W. J. Weber, D. K. Shuh, N. M. Hamdan, B. S. Mun, E. M. Adams, D. E. McCready, V. Shutthanandan, D. W. Lindle, G. Balakrishnan, D. M. Paul, E. M. Gullikson, R. C. C. Perera, J. Lian, L. M. Wang, R. C. Ewing, *Phys. Rev. B* 70 (2004) 100101.
- [14] W. Lee, M.-H. Cho, Y. Kim, J. Baeck, I. Jeong, K. Jeong, K. Chung, S. Kim, D.-H. Ko, *Thin Solid Films* 518 (2010) 1682 – 1688.
- [15] R. M. Martin, J. Boyce, J. Allen, F. Holtzberg, *Physical Review Letters* 44 (1980) 1275.
- [16] T. Kasuya (1982).
- [17] J. V. Vleck, *The Theory of Electric and Magnetic Susceptibilities*, Oxford University Press, London, 1965.
- [18] E. Suljoti, M. Nagasono, A. Pietzsch, K. Hickmann, D. M. Trots, M. Haase, W. Wurth, A. Föhlisch, *J. Chem. Phys.* 128 (2008) –.
- [19] G. Kaindl, G. Kalkowski, W. D. Brewer, B. Perscheid, F. Holtzberg, *J. Appl. Phys.* 55 (1984) 1910–1915.
- [20] B. T. Thole, G. van der Laan, J. C. Fuggle, G. A. Sawatzky, R. C. Karnatak, J.-M. Esteve, *Phys. Rev. B* 32 (1985) 5107–5118.
- [21] R. D. Cowan, *The Theory of Atomic Structure and Spectra*, University of California Press, Berkeley, CA, 1981.
- [22] H. Ogasawara, A. Kotani, *J Phys Soc Jpn* 64 (1995) 1394–1401.
- [23] Y. Takayama, M. Shinoda, K. Obu, C. Lee, H. Shiozawa, M. Hirose, H. Ishii, T. Miyahara, J. Okamoto, *J Phys Soc Jpn* 71 (2002) 340–346.
- [24] M. Rákera, *An X-ray spectroscopic study of novel materials for electronic applications*, Ph.D. thesis, University of Osnabrück, Osnabrück, 2009.